Cell Reports
Medicine

Report

β-sitosterol reduces anxiety and synergizes with established anxiolytic drugs in mice

Graphical abstract

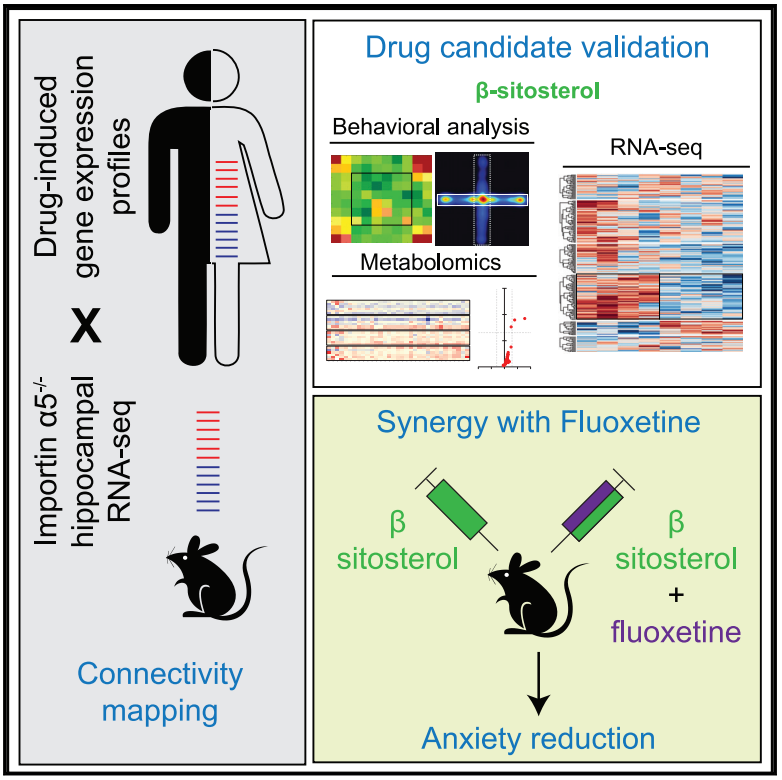

Authors

Nicolas Panayotis, Philip A. Freund, Letizia Marvaldi, ..., Tevie Mehlman, Michael M. Tsoory, Mike Fainzilber

Correspondence

nicolas.panayotis@weizmann.ac.il

In brief

Panayotis et al. identify β-sitosterol as an anxiolytic compound when administered alone and in combination with sub-efficacious doses of the SSRI fluoxetine, in both naive and chronically stressed mice. Their results suggest that β-sitosterol can be used in anxiety treatments.

Highlights

- *In silico* screen identifies β-sitosterol as a candidate anxiolytic drug
- β-sitosterol is anxiolytic in both naive and chronically stressed mice
- β-sitosterol alters the expression of immediate early genes
- Sub-efficacious doses of β-sitosterol and fluoxetine synergize when combined

Panayotis et al., 2021, Cell Reports Medicine *2*, 100281
May 18, 2021
https://doi.org/10.1016/j.xcrm.2021.100281

CellPress

Cell Reports Medicine

CellPress
OPEN ACCESS

Report

β-sitosterol reduces anxiety and synergizes with established anxiolytic drugs in mice

Nicolas Panayotis,[1,5,*] Philip A. Freund,[1] Letizia Marvaldi,[1] Tali Shalit,[2] Alexander Brandis,[3] Tevie Mehlman,[3] Michael M. Tsoory,[4] and Mike Fainzilber[1]

[1]Department of Biomolecular Sciences, Weizmann Institute of Science, Rehovot, Israel
[2]Ilana and Pascal Mantoux Institute for Bioinformatics, The Nancy and Stephen Grand Israel National Center for Personalized Medicine, Weizmann Institute of Science, Rehovot, Israel
[3]Life Science Core Facility, Weizmann Institute of Science, Rehovot, Israel
[4]Department of Veterinary Resources, Weizmann Institute of Science, Rehovot, Israel
[5]Lead contact
*Correspondence: nicolas.panayotis@weizmann.ac.il
https://doi.org/10.1016/j.xcrm.2021.100281

SUMMARY

Anxiety and stress-related conditions represent a significant health burden in modern society. Unfortunately, most anxiolytic drugs are prone to side effects, limiting their long-term usage. Here, we employ a bioinformatics screen to identify drugs for repurposing as anxiolytics. Comparison of drug-induced gene-expression profiles with the hippocampal transcriptome of an importin α5 mutant mouse model with reduced anxiety identifies the hypocholesterolemic agent β-sitosterol as a promising candidate. β-sitosterol activity is validated by both intraperitoneal and oral application in mice, revealing it as the only clear anxiolytic from five closely related phytosterols. β-sitosterol injection reduces the effects of restraint stress, contextual fear memory, and c-Fos activation in the prefrontal cortex and dentate gyrus. Moreover, synergistic anxiolysis is observed when combining sub-efficacious doses of β-sitosterol with the SSRI fluoxetine. These preclinical findings support further development of β-sitosterol, either as a standalone anxiolytic or in combination with low-dose SSRIs.

INTRODUCTION

Currently available treatments for anxiety and stress-related disorders rely heavily on the pharmacological modulation of hormones and neurotransmitter systems.[1–3] The suboptimal efficacy and side-effect profiles of current anxiolytics have motivated a search for new targets and drug candidates in this area.[4,5] Intracellular transport pathways, especially those that impact nucleocytoplasmic shuttling, are an emerging source of new druggable targets in multiple diseases.[6–8] Importins are the main nucleocytoplasmic transport factors, with roles ranging from nuclear import per se to the long-distance trafficking of cargos from the synapse or the axon to the nucleus.[9–11] We recently screened a battery of importin α mutant mouse lines for behavioral phenotypes and identified a specific role of importin α5 in anxiety[12] and importin α3 in chronic pain.[13]

Importin α5 knockout or specific knockdown in the hippocampus caused a significant reduction of anxiety-related behaviors[12]; hence, we sought to identify drug candidates that mimic this effect. The connectivity map (CMap) database[14] allows the comparison of transcriptome profiles of interest to gene-expression profiles from cultured human cell lines treated with thousands of clinically approved compounds.[15] We used this approach to identify similarities between the importin α5 knockout mouse hippocampal transcriptome and gene-expression changes induced by small molecules. This report describes the use of CMap to identify β-sitosterol as a candidate anxiolytic, validation and specificity of the anxiolysis activity, and characterization of a striking anxiolytic synergy between this phytosterol and the established drug fluoxetine.

RESULTS

We queried CMap with an ensemble of differentially expressed genes from the mouse importin $\alpha5^{-/-}$ hippocampus (Figure 1A). As noted above, such analyses identify approved drugs that may mimic the desired activity due to similarities with the query transcriptome profile. We indeed found drug candidates with high CMap scores (>0.75, Table S1). We further limited the top candidates to those with penetrability across the blood-brain barrier, the possibility of oral delivery, and limited likelihood of side effects (Figure 1B). Five compounds met these criteria, namely, β-sitosterol, oxamniquine, fluspirilene, primaquine, and alvespimycin. We screened for possible anxiolytic properties of these compounds by intraperitoneal (i.p.) injection of each drug or its vehicle, 1 h before an open-field (OF) test. β-sitosterol was the only compound with clear anxiolytic activity under these experimental conditions, significantly increasing the distance traveled, the number of visits, and the number of rearings in the central (i.e., anxiogenic) area of the OF (Figure 1C; Table S2). Fluspirilene

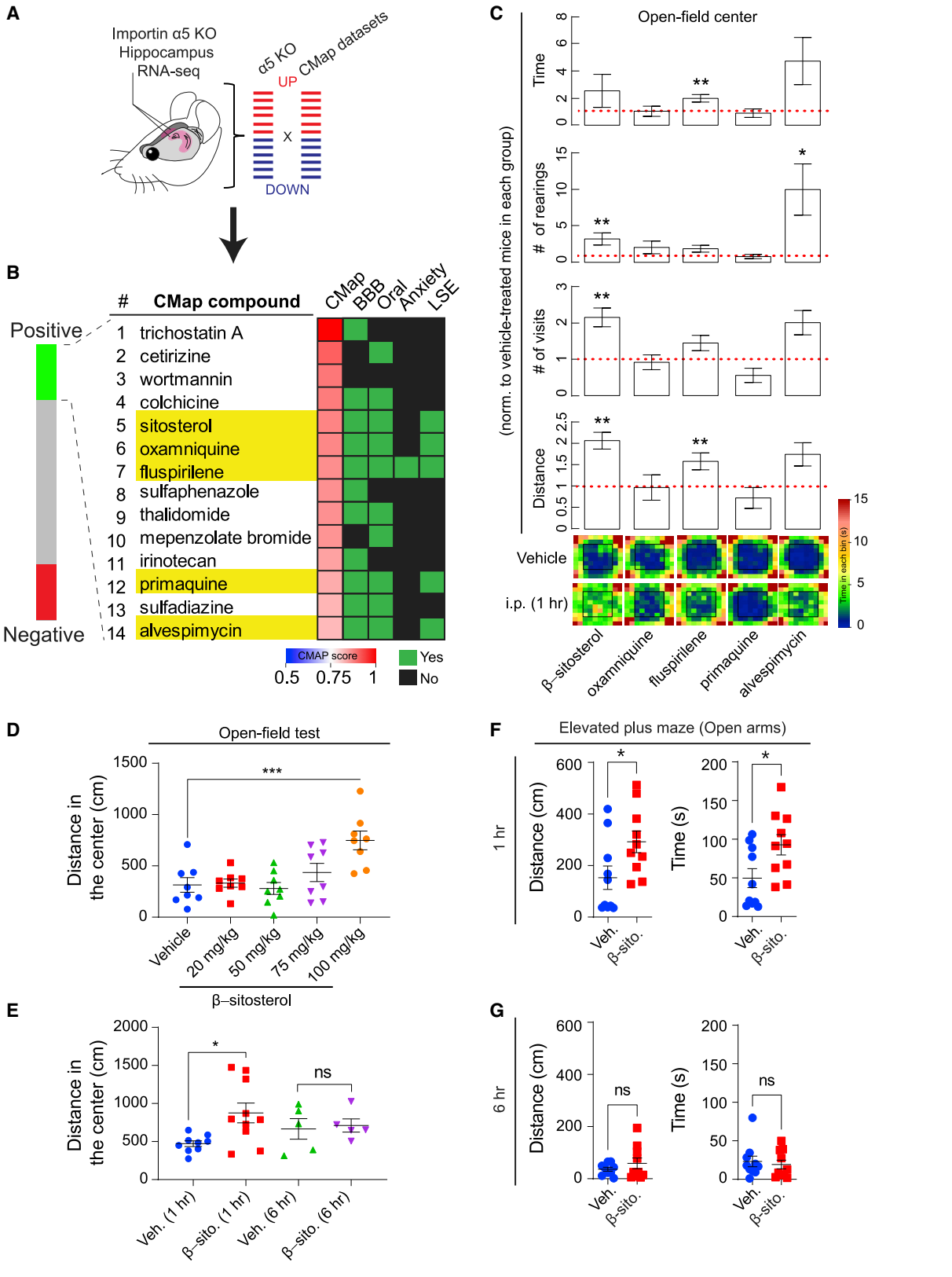

(legend on next page)

increased both the distance and the time spent in the center area. In contrast, none of the three other candidates reliably influenced anxiety-related measures (Figure 1C; Table S2).

We defined the minimal anxiolytic β-sitosterol dosage through dose-response and therapeutic window experiments, using both oral gavage and intraperitoneal administration regimens. The results in male mice show that β-sitosterol induces robust anxiolytic effects at a dose of 100 mg/kg 1 h after injection (Figures 1D and 1E; Figures S1A and S1B). Using the elevated plus maze (EPM), we confirmed that, 1 h after injection, 100 mg/kg β-sitosterol elicited anxiolytic responses, significantly increasing the distance traveled and time spent in the EPM open arms (Figure 1F). In contrast, no significant effects were observed after 6 h (Figure 1G). Moreover, β-sitosterol did not affect animal movement velocity during the test session (Figures S1A and S1B). We further assessed balance and coordination in the rotarod test and both mechanical and thermal sensitivity using the von Frey and heat probe tests. The results show that at 1 h after injection, β-sitosterol-treated animals behaved as their vehicle-treated littermates (Figures S1C–S1E), highlighting the specificity of the anxiolytic effect. We also tested the effects of β-sitosterol in female mice, using the EPM. The results were more variable (Figure S1F) and did not reach statistical significance, possibly due to known effects of the estrus cycle on anxiety-related behaviors and anxiolytics' efficacy.[16] We used the male mice data and FDA recommendations[17,18] to calculate the human equivalent dose (HED) as 486 mg and the recommended starting dose as 48.6 mg (considering a standard body weight of 60 kg). This dosage is well in the range (~2 g per day) of plant sterol dietary supplementation typically administered for cholesterol management.[19]

Plant sterols (phytosterols) such as β-sitosterol are cholesterol-based compounds used as "nutraceuticals" in some indications, primarily hypercholesterolemia.[20] There are several closely related phytosterols; hence, we also evaluated the activity of stigmasterol, campesterol, brassicasterol, and fucosterol in the OF (Figure 2). Surprisingly, despite the high structural similarities among all the tested sterols, only β-sitosterol reliably affected all OF anxiolysis measures compared to the vehicle group (Figures 2B and 2C). Fucosterol and brassicasterol had effects on only one or two of the test parameters, respectively (Figure S1C). Stigmasterol and campesterol did not influence any anxiety measures, despite the high doses tested (Figure 2; Figure S1C). Hence, β-sitosterol is the only phytosterol from those tested that induced robust anxiolytic effects.

To characterize the molecular determinants of β-sitosterol-induced anxiolysis, we carried out RNA sequencing (RNA-seq) analyses from hippocampi extracted 1 and 6 h after i.p. injection of β-sitosterol or the non-anxiolytic stigmasterol. There was little or no overlap in the differentially expressed gene sets between β-sitosterol and stigmasterol treatments, further emphasizing the specific effects of β-sitosterol (Figure 3; Figure S2; Table S3). β-sitosterol had no effect on expression levels of importin α family members, in line with the expectation that CMap drug candidates will likely mimic importin function perturbation, rather than acting as importin expression inhibitors. K-means clustering (k = 6) further revealed a set of 54 genes (Figure 3B), which were particularly deregulated 1 h after β-sitosterol treatment, and hence are likely to represent a molecular signature of the anxiolytic response. These genes include rapid-response genes such as *Fos*, *Arc*, *Npas4*, and *Dusp1*. Ingenuity Pathway analyses of the datasets further highlighted immediate early gene (IEG) networks regulated by 1 h β-sitosterol treatment (Figure 3B; Table S3). Indeed, previous reports have associated hippocampal *Fos* deficits with reduced anxiety and an altered response to chronic stress in mice.[21,22] Moreover, while higher *Npas4* mRNA levels have been observed after stress exposure,[23] *Npas4*-null mice were described to be less anxious than wild-type and heterozygous littermates.[24,25] *Fos* is a biomarker for anxiety in the amygdala (AMY), the hippocampus (HPC), and the bloodstream.[26] It has been shown that memory-linked *Fos*-expressing neurons recruit excitatory inputs and promote memory generalization, whereas memory-linked *Npas4*-expressing neurons recruit inhibitory inputs and promote memory discrimination in the dentate gyrus (DG).[27] As for *Arc* and *Dusp1*, their respective knockouts revealed reduced anxiety-related responses in mice.[28,29] Prefrontal cortex (PFC) or HPC inactivation during contextual fear conditioning reduces freezing and IEG expression, leading to the suggestion that PFC-HPC connections are partially responsible for contextual learning.[30]

To further explore the downregulation of *Fos* following β-sitosterol injection, mice underwent contextual fear conditioning. The

Figure 1. *In silico* screening for anxiolytic compounds mimicking the importin α5 mutant phenotype

(A) The CMap approach was used to compare DEGs from hippocampal RNA-seq analysis of importin α5 knockouts to DEGs from cell lines treated with drugs and drug candidates.

(B) Compounds functionally related to the query state (CMap score >0.75). The candidate compounds were prioritized based on lack of a prior indication for anxiety, ability to cross the blood-brain barrier, compatibility with oral application, and low likelihood of side effects (LSE).

(C) The top five drugs meeting these criteria were tested for anxiolytic properties in mice using the open-field test 1 h after i.p. injection, as compared to vehicle. The time spent, the number of rearings, the number of visits, and the distance traveled in the open-field center are represented normalized to vehicle treatment values for each group. Data are shown for β-sitosterol (100 mg/kg), n = 5, vehicle, n = 8; alvespimycin (75 mg/kg), n = 10, vehicle, n = 10; oxamniquine (15 mg/kg), n = 5, vehicle, n = 5; fluspirilene (10 mg/kg), n = 8, vehicle, n = 7 and primaquine (60 mg/kg) n = 5, vehicle, n = 5. The bottom panel depicts group heatmap representations of mouse activity over 10 min of open-field exploration. See Table S2 for raw data analysis.*p < 0.05, **p < 0.01; two-tailed t test, mean ± SEM

(D and E) β-sitosterol was further studied for its ability to reduce anxiety when given by oral gavage, in both dose-response and time window experiments. The compound showed significant anxiolytic properties in the open-field test at a dosage of 100 mg/kg and 1 h after its administration (D: n = 8 mice per dosage, 1-way ANOVA followed by Dunnett's multiple-comparisons test with the vehicle group as control; E: β-sitosterol, n = 10, vehicle, n = 9 mice at 1 h and n = 5 mice in both groups at 6 h, 2-way ANOVA followed by Sidak's multiple-comparisons test); *p < 0.05, **p < 0.01, ***p < 0.001; mean ± SEM.

(F and G) β-sitosterol effects were studied in the elevated plus maze. The compound showed significant anxiolytic properties at a dosage of 100 mg/kg (i.p) 1 h after its administration (F) and no effects when tested 6 h after injection (G). (F and G: β-sitosterol, n = 10, vehicle, n = 10 mice in each time points, two-tailed t test; *p < 0.05; mean ± SEM). See also Figure S1.

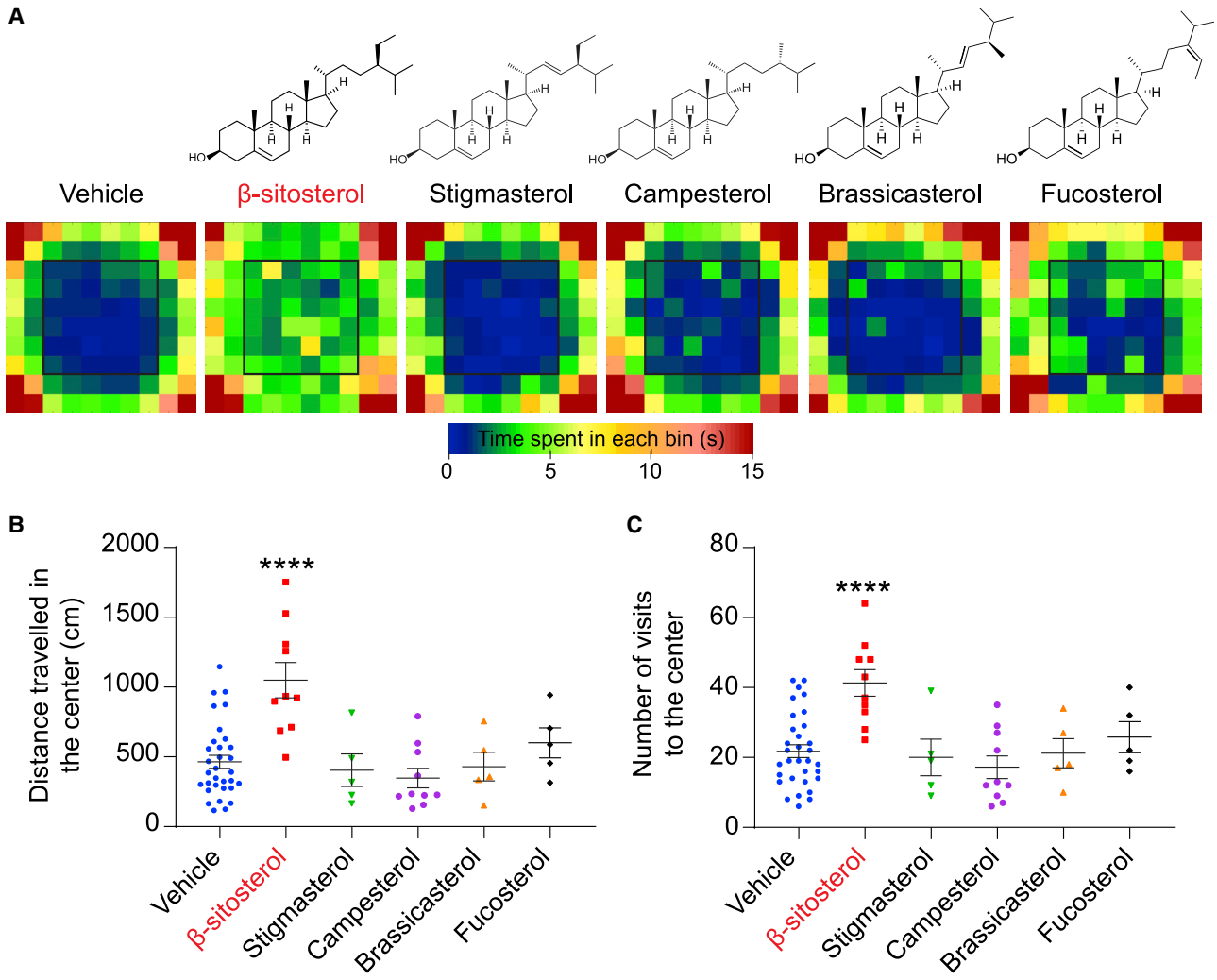

Figure 2. Comparison of the anxiolytic activities of plant sterols

(A) Chemical structures of β-sitosterol, stigmasterol, campesterol, brassicasterol, and fucosterol. All phytosterols were diluted in corn oil (vehicle) and administered intraperitoneally at a final dosage of 100 mg/kg, 1 h before evaluation of anxiolytic effects in the open-field test. The bottom panel depicts group heatmap representations of mouse activity over 10 min of open-field exploration.

(B and C) β-sitosterol was the only compound tested that caused a significant increase in the distance traveled (B) and the number of visits in the open-field center (C) compared to vehicle-treated mice. Vehicle, n = 32; β-sitosterol, n = 10; stigmasterol, n = 5; campesterol, n = 10; brassicasterol, n = 5; fucosterol, n = 5. The effect of the different sterols on the OF center exploration was analyzed by a 1-way ANOVA followed by Dunnett's multiple-comparisons test with the vehicle group as control. ***$p < 0.0001$, mean ± SEM. See also Figure S1.

protocol consisted of three phases: habituation, acquisition/conditioning (two pairings of tone with foot shock), and a final context test (Figure 3C). Mice received i.p. injections containing either β-sitosterol or a control vehicle 1 h before placement in the conditioning chamber. The mice were sacrificed and their brains were dissected 1 h following the context test. There was no significant difference in distance traveled (cm) and freezing duration (s) between β-sitosterol and vehicle conditions in the acquisition/conditioning phase (Figure S2D); however, β-sitosterol-injected mice had a significantly shorter cumulated freezing duration (s) compared to vehicle-injected mice (vehicle, 285.1 s ± 3.79; β-sitosterol, 263.2 s ± 6.16; $p < 0.01$), implying a mild reduction in contextual fear (Figure 3D). Slices containing the PFC, HPC, and AMY were extracted and stained for c-Fos and DAPI. c-Fos levels were significantly lower in the PFC and the dentate gyrus of β-sitosterol-injected mice compared to vehicle-injected mice (Figures 3E–3G); however, there was no significant c-Fos reduction in the CA3 or the AMY (Figures S2E–S2G). These results show that β-sitosterol reduces c-Fos expression and that this reduction occurs in brain regions involved in contextual fear memory such as the PFC and the HPC. IEGs represent strong candidates for future investigation as their deregulation can reflect perturbations of neuronal activity at the circuit level.

We next sought to examine potential interactions between β-sitosterol and known anxiolytic drugs. β-sitosterol is a dietary component present in plants, grains, cereals, and fruits[31] and is

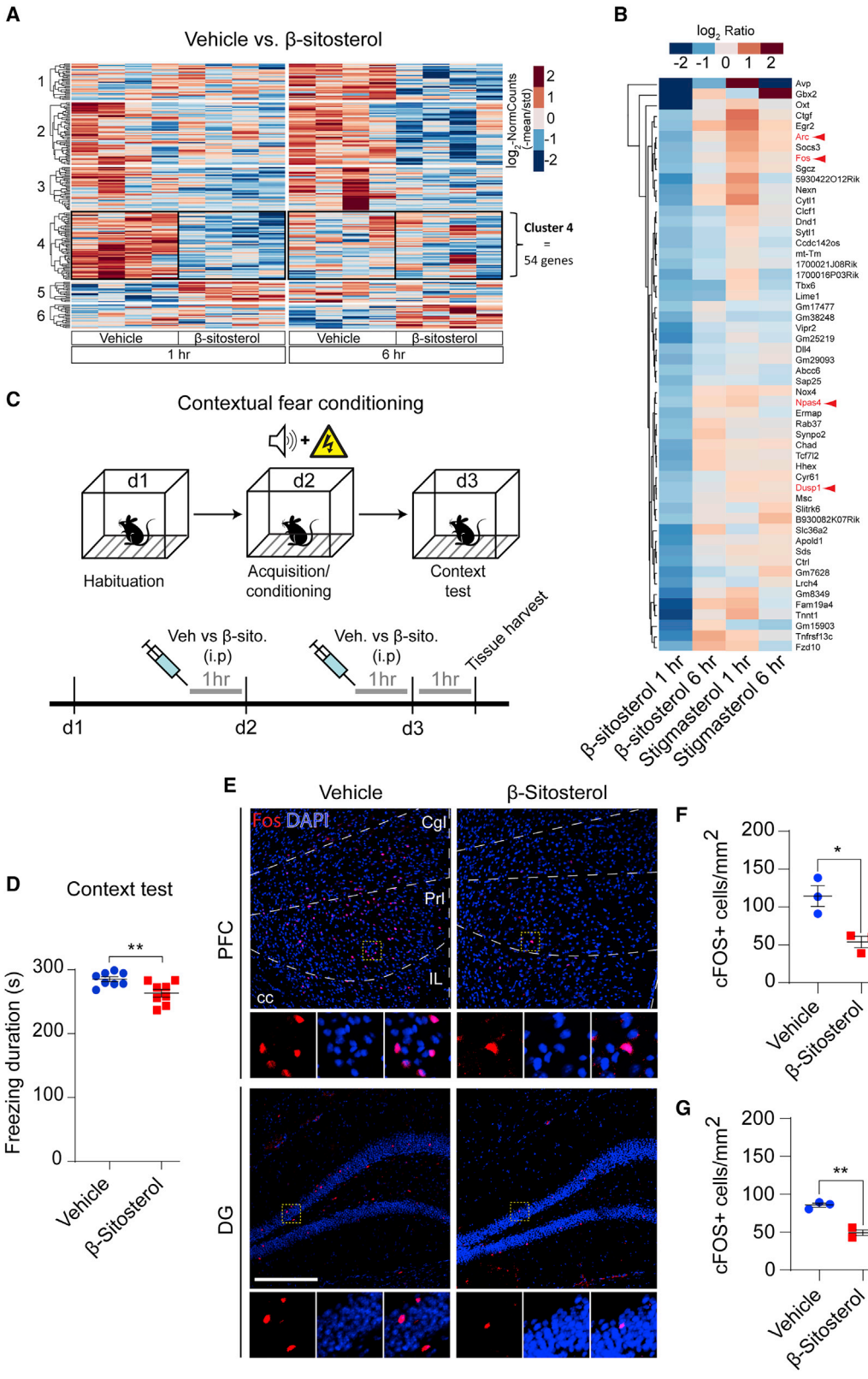

(legend on next page)

widely marketed and taken in high doses as a nutraceutical.[32] Given this favorable safety profile, we asked whether co-administration of β-sitosterol with conventional anxiolytic drugs such as fluoxetine[33] might serve to reduce dose requirements and minimize possible side effects of fluoxetine. A dose-response analysis with fluoxetine showed that doses of 10 mg/kg and above had significant anxiolytic effects in mice, while doses of 5 mg/kg and below had no apparent effect (Figure S3), in agreement with the literature.[34] We then tested the effect of increasing the β-sitosterol dose in mice receiving a sub-efficacious dose of 5 mg/kg fluoxetine (Figure 4). Strikingly, we observed a synergistic effect of sub-efficacious dosage combinations comprising 5 mg/kg fluoxetine with 10, 20, or 50 mg/kg β-sitosterol (Figures 4A–4C; Figure S3E). We further assessed the potential of such a combination on chronically stressed animals. To do so we compared the effects of three weeks of restraint stress in mice treated with vehicle, fluoxetine (20 mg/kg), β-sitosterol (100 mg/kg), or the combination 5 mg/kg fluoxetine/20 mg/kg β-sitosterol to naive mice (subjected to no stress or treatments) in the novelty-suppressed feeding test of hyponeophagia.[35] The results show that compared to naive mice, restraint-stressed animals receiving the vehicle accessed the food with a significant delay (Figure 4E). In contrast, treatment with 20 mg/kg fluoxetine, 100 mg/kg β-sitosterol, or the combination of both (5 mg/kg fluoxetine/20 mg/kg β-sitosterol) accessed the food as fast as the naive control mice (Figure 4E). These findings suggest that combination treatments with β-sitosterol and selective serotonin reuptake inhibitor (SSRI) family anxiolytics may provide therapeutic effects at a low dosage, thus reducing the potential for undesirable SSRI side effects.

To examine regional differences in major neurotransmitter and amino acid concentrations, liquid chromatography coupled with tandem mass spectrometry (LC-MS/MS) was performed on micropunches extracted from the PFC, caudate-putamen (CPu), hypothalamus (HPTH), HPC, amygdala (AMY), and substantia nigra (SN) of WT mice treated with 100 mg/kg β-sitosterol or a control vehicle injection (Figures 4F and 4G). Changes in compound concentration with a $\log_2$ fold change >0.58 were considered significant at $p < 0.05$ (Figures 4H and 4I; Figure S4A; Table S4). Dopamine (DA), Thr, Ala, and Citrulline concentrations were significantly lower in the PFC after β-sitosterol compared to vehicle injections (Figure 4H). Additionally, Trp, Met, and Tyr concentrations were lowered in the HPC (Figure 4I). There were no significant changes in compound concentration in the CPu, HPTH, AMY, or SN (Figure S4A). Altogether, the results suggest that acute β-sitosterol injection can decrease neurotransmitter and amino acid concentration in selected brain regions.

Several of these significantly affected metabolites have been related to anxiety and/or stress modulation in the literature. For instance, exposure of rodents to anxiogenic/stressful protocols was shown to cause aberrant PFC neuronal activity and a specific elevation of DA in the PFC.[36] In the brain, the neuronal NO synthase (nNOS), responsible for the conversion of arginine to citrulline, is enriched in brain areas related to stress disorders,[37] and NO levels are elevated in the plasma of rats under chronic stress.[38] NO synthesis inhibition in the PFC[39] was shown to have antidepressant effects. Interestingly, the nNOS inhibitor 7-NI and SSRIs such as fluoxetine and venlafaxine attenuate stress-induced c-Fos expression in overlapping brain areas including the PFC.[40]

To examine the synergistic effects of sub-efficacious doses of β-sitosterol and fluoxetine at the neurochemical level, the above experiment was repeated with the treated animals receiving both fluoxetine (5 mg/kg, i.p. for 3 weeks) and β-sitosterol (20 mg/kg, i.p. 1 h before tissue sampling), compared to animals receiving the respective vehicles. LC-MS/MS analysis revealed that the combination treatment resulted in a significant elevation of 5-HT concentrations in the PFC, NE in the PFC and CPu, and DA in the HPC along with Val, Phe, Tyr, and Trp in the SN (Figures 4J–4M), while none of the investigated metabolites were altered in the HPTH or AMY (Figure S4D). Thus, the combination of β-sitosterol and fluoxetine at sub-efficacious doses elicits specific pro-serotonergic and catecholaminergic responses in brain regions relevant for anxiety regulation that were not observed after treatment with 5 mg/kg fluoxetine alone (Figure 4G; Figure S4B). This complements and strengthens our finding that the combined treatment is synergic for anxiety reduction.

DISCUSSION

The current study identifies acute anxiolytic activity of β-sitosterol and describes synergistic effects when β-sitosterol is co-administered with the SSRI fluoxetine. While these results highlight the possibility of clinically testing such a combination, elucidation of the mechanisms linking the pharmacological pathways warrants further investigation. In this context, it is noteworthy that others have reported sensitivity of the human serotonin transporter SERT to membrane cholesterol concentration.[41,42] More recently, a paper proposed a model whereby fluoxetine might interact with a cholesterol-interaction motif in the BDNF receptor TrkB to induce anti-depressant effects.[43] In

Figure 3. Effects of β-sitosterol treatment on gene expression in mouse hippocampus

(A) Heatmap representation of standardized $\log_2$-normalized counts of DEGs after β-sitosterol treatment (n = 4 mice/group, 2 groups: 1 h, 6 h after 100 mg/kg β-sitosterol i.p. injection). K-means clustering analysis revealed a specific pattern of gene downregulation in cluster 4 at 1 h after treatment.

(B) Heatmap based on gene sets of cluster 4, Log_2 ratio of treated (drug) versus untreated (vehicle) is represented. A clear pattern of downregulation in the sitosterol 1 h condition not visible after 6 h or under stigmasterol treatment (see Figure S2).

(C) Timeline and schematic representation of the contextual fear conditioning experiment. Gray bars indicate 1 h intervals. On the second day (acquisition phase) and third day (context test), animals were injected with β-sitosterol (100 mg/kg, i.p.) or its vehicle solution (corn oil) 1 h before the experiment. After completion of the context test on day 3, brains were harvested for immunohistochemistry.

(D) Total freezing duration in the context text. n = 8 mice per group. **p < 0.01; two-tailed t test. Mapping of c-Fos activated neurons *in vivo*.

(E) Representative images of the prefrontal cortex (PFC) and the dorsal dentate gyrus (DG). Scale bar, 200 μm.

(F and G) Quantifications of the number of c-Fos-positive neurons in the PFC (F) and the DG (G) after contextual fear conditioning. n = 3 mice per group.

*p < 0.05; **p < 0.01; two-tailed t test, mean ± SEM. See also Figure S2.

CellPress
OPEN ACCESS

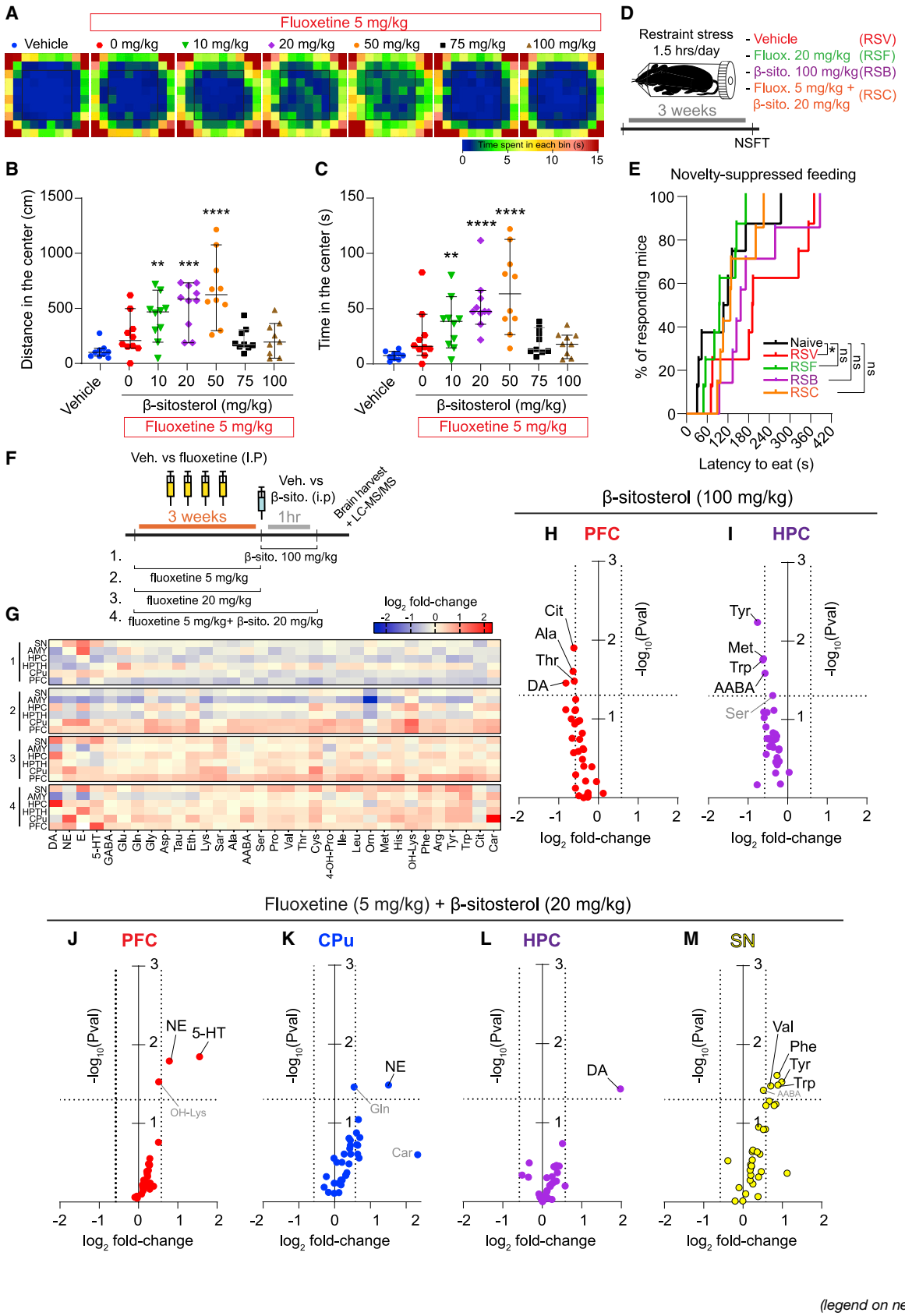

(legend on next page)

addition, studies suggested associations between the use of SSRIs and altered levels of cholesterol.[44,45] Thus, it would be interesting to assess in the future whether β-sitosterol-related changes in membrane lipid configuration can potentiate fluoxetine-SERT interactions or fluoxetine-TrkB signaling. The different responsiveness of male versus female mice to β-sitosterol should also be examined in more detail, specifically the likely influence of estrus cycle or other hormonal events on the anxiolytic response.[16] Finally, the effects of chronic treatment with β-sitosterol remain to be elucidated and due to the hydrophobic nature of the drug will likely require testing by long-term supplementation in animal diets.

There is a pressing need for new drugs to treat anxiety and stress-related disorders; however, the discovery and development of such compounds remains a significant challenge.[2,5] Phytosterols are close analogs of cholesterol and are found in a variety of edible plants,[20,31,46] with advantageous safety profiles and history of usage in humans.[47,48] Phytosterols can affect several biological processes through neuroprotective and antioxidative activity,[20] but their impact on brain functions is not well understood. On the one hand, a mouse model with vastly increased phytosterol levels from birth did not present any apparent memory or anxiety phenotypes,[49] while, on the other hand, several studies have reported pro-explorative or antidepressant properties of crude or partly purified plant sterols when administered intraperitoneally.[50–52] Our findings establish β-sitosterol as the only specific and robust anxiolytic from a battery of closely related phytosterols, providing a possible explanation for the conflicting reports on activities of mixed phytosterol extracts summarized above. Moreover, we show that β-sitosterol can synergize with subtherapeutic doses of the SSRI fluoxetine. These findings suggest that β-sitosterol can be repositioned as an anxiolytic, either as a standalone therapeutic or in a synergic combination with SSRI class drugs such as fluoxetine.

Limitations of study

The present study used an *in silico* screen to identify β-sitosterol as an anxiolytic compound. While our data showed a robust effect in male mice, we observed a significant variability of the response to β-sitosterol in adult female mice, perhaps due to effects of the estrus cycle on anxiety and depression-related behaviors and the efficacy of antidepressants. Hence, future conclusive determination of the anxiolytic properties of β-sitosterol in females will require estrus stage coordination and a large number of mice. Moreover, we did not fully elucidate the molecular mechanisms underlying β-sitosterol's anxiolytic effects, either alone or in combination with SSRIs. The acute anxiolytic effects of β-sitosterol directed our attention to rapidly induced genes; however, we cannot rule out the involvement of other differentially expressed genes in this anxiolytic mechanism. In addition, further functional assessments will be necessary to ascertain the mechanism of action of β-sitosterol at the synaptic and/or circuit level. Finally, our strategy for administering β-sitosterol (oral gavage or IP injection) limited the time course of study. Testing for long-term effects of β-sitosterol will require paradigms of chronic administration that are not confounded by the stress of repeated injections or gavages. Since the compound is not readily water soluble, this will require long-term provision and monitored consumption of sitosterol-enriched diets.

STAR★METHODS

Detailed methods are provided in the online version of this paper and include the following:

- KEY RESOURCES TABLE
- RESOURCE AVAILABILITY
  - Lead contact
  - Materials availability
  - Data and code availability
- EXPERIMENTAL MODEL AND SUBJECT DETAILS
  - Animal subjects
  - Study approval
- METHOD DETAILS
  - Pharmacological treatments
  - Behavioral analysis

Figure 4. Fluoxetine synergizes with β-sitosterol for anxiolysis in mice

The effect of fluoxetine/β-sitosterol co-treatments was studied by injecting mice with 5 mg/kg fluoxetine (daily i.p. injection for 3 weeks) and then the indicated doses of β-sitosterol (1 h before the test). Control littermates received both vehicles (saline and corn-oil) only.

(A) Group heatmap representations of mouse activity over 10 min of open-field exploration.

(B and C) Distance traveled (B) and time spent (C) in the open-field center (in cm) monitored over 10 min in the open-field test for vehicle-injected animals (vehicle, n = 9) and mice receiving one of the 6 combinations as indicated ($n \geq 9$ per combination). The effects on OF center exploration in (B) and (C) were analyzed by a two-sided Kruskal-Wallis test with vehicle as control. *$p < 0.05$, **$p < 0.01$, ***$p < 0.001$, ****$p < 0.0001$. Error bars represent the median with a 95% confidence interval (CI). See also Figure S3.

(D and E) Mice were subjected to 1.5 h restraint stress for 3 weeks and treated with vehicle (RSV), fluoxetine 20 mg/kg (RSF), β-sitosterol 100 mg/kg (RSB), or the combination of fluoxetine 5 mg/kg + β-sitosterol 20 mg/kg (RSC) and compared to naive mice in the novelty-suppressed feeding test (NSFT). Data are expressed as the cumulative percentage of animals that have eaten (latency to eat, in seconds), over the test session (naive, n = 10; RSF, n = 10; RSB, n = 9; RSC, n = 10). Data were analyzed using the Mantel-Cox log-rank test with the naive group set as the control. *$p < 0.05$.

(F) Timeline and schematic representation of the different drug treatments preceding the LC-MS/MS experiment.

(G) Heatmap representation of the metabolite levels (expressed as a log2 fold change between vehicle and treated mice) in each of the four conditions: β-sitosterol 100 mg/kg (1), fluoxetine 5 mg/kg (2), fluoxetine 20 mg/kg (3), and the combination fluoxetine 5 mg/kg + β-sitosterol 20 mg/kg (4).

(H and I) Volcano plot representations of the neurochemical alterations induced by the 100 mg/kg β-sitosterol treatment (i.p.) in the PFC (H) and the HPC (I).

(J)–(M) Volcano plot representations of the neurochemical alterations induced by a treatment combining fluoxetine (5 mg/kg, daily i.p. injection for 3 weeks) and β-sitosterol (20 mg/kg, 1 h before the test, i.p.) in the PFC (J), the CPu (K), the HPC (L), and the SN (M).

For results from (H)–(M), changes in compound concentration when the $\log_2$ fold change (vehicle versus β-sitosterol) >0.58 were considered significant at $p < 0.05$ (represented on the plot as $-\log_{10}$(p value) >1.3). See also Figure S4 and Table S4.

- Chronic restraint stress
- Open field test
- Elevated plus maze
- Contextual fear conditioning
- Novelty-suppressed feeding
- Accelerated rotarod
- Heat probe test
- von Frey test
- RNA expression analysis (RNA-seq)
- Library construction and sequencing
- Sequence data analysis
- Stigmasterol injection
- Bioinformatics analysis
- Connectivity Map analysis
- Immunofluorescence
- Image processing and quantification
- Quantification of c-Fos positive neurons
- Neurochemical measurements
- Extraction
- Derivatization
- LC-MS/MS analysis

● QUANTIFICATION AND STATISTICAL ANALYSIS

- Data collection
- Statistics

SUPPLEMENTAL INFORMATION

Supplemental information can be found online at https://doi.org/10.1016/j.xcrm.2021.100281.

ACKNOWLEDGMENTS

We thank Tony Futerman and Dalia Gordon for helpful comments and discussions. We are indebted to Nitzan Korem, Nataliya Okladnikova, and Hadar Reisin-Tzur for excellent professional and technical assistance and Yaniv Levi for devoted assistance with animal care. This research was supported by the European Research Council (PoC FAITh), the Nella and Leon Benoziyo Center for Neurological Diseases, the Chaya Professorial Chair in Molecular Neuroscience (M.F.), the Koshland Senior Postdoctoral fellowship and the Israel Ministry of Immigrant Absorption (N.P.), and the Carolito Stiftung Research Fellow Chair in Neurodegenerative Diseases (M.M.T.).

AUTHOR CONTRIBUTIONS

N.P. performed behavioral, molecular, imaging, and pharmacological experiments. T.S. performed RNA-seq data and bioinformatics analysis. A.B. and T.M. performed the neurochemical measurements. N.P., A.B., M.M.T., and M.F. contributed to the concept and design of the experiments. N.P., P.A.F., L.M., T.S., A.B., and T.M. collected, analyzed, or interpreted the data. N.P. and M.F. guided research and wrote the manuscript, with input from all coauthors.

DECLARATION OF INTERESTS

N.P. and M.F. have a patent application related to this work, PCT patent application number PCT/IL2018/050495, Publication number WO/2018/207178, on "Methods of treating psychiatric stress disorders."

Received: September 24, 2020
Revised: January 28, 2021
Accepted: April 22, 2021
Published: May 18, 2021

REFERENCES

1. Dias, B.G., Banerjee, S.B., Goodman, J.V., and Ressler, K.J. (2013). Towards new approaches to disorders of fear and anxiety. Curr. Opin. Neurobiol. *23*, 346–352.
2. Griebel, G., and Holmes, A. (2013). 50 years of hurdles and hope in anxiolytic drug discovery. Nat. Rev. Drug Discov. *12*, 667–687.
3. Murrough, J.W., Yaqubi, S., Sayed, S., and Charney, D.S. (2015). Emerging drugs for the treatment of anxiety. Expert Opin. Emerg. Drugs *20*, 393–406.
4. Calhoon, G.G., and Tye, K.M. (2015). Resolving the neural circuits of anxiety. Nat. Neurosci. *18*, 1394–1404.
5. Hariri, A.R., and Holmes, A. (2015). Finding translation in stress research. Nat. Neurosci. *18*, 1347–1352.
6. Mahipal, A., and Malafa, M. (2016). Importins and exportins as therapeutic targets in cancer. Pharmacol. Ther. *164*, 135–143.
7. Mor, A., White, M.A., and Fontoura, B.M. (2014). Nuclear trafficking in health and disease. Curr. Opin. Cell Biol. *28*, 28–35.
8. Kosyna, F.K., and Depping, R. (2018). Controlling the Gatekeeper: Therapeutic Targeting of Nuclear Transport. Cells *7*, E221.
9. Panayotis, N., Karpova, A., Kreutz, M.R., and Fainzilber, M. (2015). Macromolecular transport in synapse to nucleus communication. Trends Neurosci. *38*, 108–116.
10. Miyamoto, Y., Yamada, K., and Yoneda, Y. (2016). Importin α: a key molecule in nuclear transport and non-transport functions. J. Biochem. *160*, 69–75.
11. Terenzio, M., Schiavo, G., and Fainzilber, M. (2017). Compartmentalized signaling in neurons: from cell biology to neuroscience. Neuron *96*, 667–679.
12. Panayotis, N., Sheinin, A., Dagan, S.Y., Tsoory, M.M., Rother, F., Vadhvani, M., Meshcheriakova, A., Koley, S., Marvaldi, L., Song, D.A., et al. (2018). Importin α5 Regulates Anxiety through MeCP2 and Sphingosine Kinase 1. Cell Rep. *25*, 3169–3179.e7.
13. Marvaldi, L., Panayotis, N., Alber, S., Dagan, S.Y., Okladnikov, N., Koppel, I., Di Pizio, A., Song, D.A., Tzur, Y., Terenzio, M., et al. (2020). Importin α3 regulates chronic pain pathways in peripheral sensory neurons. Science *369*, 842–846.
14. Musa, A., Ghoraie, L.S., Zhang, S.D., Glazko, G., Yli-Harja, O., Dehmer, M., Haibe-Kains, B., and Emmert-Streib, F. (2018). A review of connectivity map and computational approaches in pharmacogenomics. Brief. Bioinform. *19*, 506–523.
15. Lamb, J., Crawford, E.D., Peck, D., Modell, J.W., Blat, I.C., Wrobel, M.J., Lerner, J., Brunet, J.P., Subramanian, A., Ross, K.N., et al. (2006). The Connectivity Map: using gene-expression signatures to connect small molecules, genes, and disease. Science *313*, 1929–1935.
16. Yohn, C.N., Shifman, S., Garino, A., Diethorn, E., Bokka, L., Ashamalla, S.A., and Samuels, B.A. (2020). Fluoxetine effects on behavior and adult hippocampal neurogenesis in female C57BL/6J mice across the estrous cycle. Psychopharmacology (Berl.) *237*, 1281–1290.
17. USFDA. Estimating the Maximum Safe Starting Dose in Initial Clinical Trials for Therapeutics in Adult Healthy Volunteers. 2005.
18. Nair, A.B., and Jacob, S. (2016). A simple practice guide for dose conversion between animals and human. J. Basic Clin. Pharm. *7*, 27–31.
19. Law, M.R. (2000). Plant sterol and stanol margarines and health. West. J. Med. *173*, 43–47.
20. Vanmierlo, T., Bogie, J.F.J., Mailleux, J., Vanmol, J., Lütjohann, D., Mulder, M., and Hendriks, J.J. (2015). Plant sterols: Friend or foe in CNS disorders? Prog. Lipid Res. *58*, 26–39.
21. McQuade, J.M., Tamashiro, K.L., Wood, G.E., Herman, J.P., McEwen, B.S., Sakai, R.R., Zhang, J., and Xu, M. (2006). Deficient hippocampal c-fos expression results in reduced anxiety and altered response to chronic stress in female mice. Neurosci. Lett. *403*, 125–130.

22. Schoenfeld, T.J., McCausland, H.C., Sonti, A.N., and Cameron, H.A. (2016). Anxiolytic Actions of Exercise in Absence of New Neurons. Hippocampus *26*, 1373–1378.

23. Drouet, J.B., Peinnequin, A., Faure, P., Denis, J., Fidier, N., Maury, R., Buguet, A., Cespuglio, R., and Canini, F. (2018). Stress-induced hippocampus Npas4 mRNA expression relates to specific psychophysiological patterns of stress response. Brain Res. *1679*, 75–83.

24. Jaehne, E.J., Klarić, T.S., Koblar, S.A., Baune, B.T., and Lewis, M.D. (2015). Effects of Npas4 deficiency on anxiety, depression-like, cognition and sociability behaviour. Behav. Brain Res. *281*, 276–282.

25. Klarić, T.S., Jaehne, E.J., Koblar, S.A., Baune, B.T., and Lewis, M.D. (2017). Alterations in anxiety and social behaviour in Npas4 deficient mice following photochemically-induced focal cortical stroke. Behav. Brain Res. *316*, 29–37.

26. Le-Niculescu, H., Balaraman, Y., Patel, S.D., Ayalew, M., Gupta, J., Kuczenski, R., Shekhar, A., Schork, N., Geyer, M.A., and Niculescu, A.B. (2011). Convergent functional genomics of anxiety disorders: translational identification of genes, biomarkers, pathways and mechanisms. Transl. Psychiatry *1*, e9.

27. Sun, X., Bernstein, M.J., Meng, M., Rao, S., Sørensen, A.T., Yao, L., Zhang, X., Anikeeva, P.O., and Lin, Y. (2020). Functionally Distinct Neuronal Ensembles within the Memory Engram. Cell *181*, 410–423.e17.

28. Duric, V., Banasr, M., Licznerski, P., Schmidt, H.D., Stockmeier, C.A., Simen, A.A., Newton, S.S., and Duman, R.S. (2010). A negative regulator of MAP kinase causes depressive behavior. Nat. Med. *16*, 1328–1332.

29. Penrod, R.D., Kumar, J., Smith, L.N., McCalley, D., Nentwig, T.B., Hughes, B.W., Barry, G.M., Glover, K., Taniguchi, M., and Cowan, C.W. (2019). Activity-regulated cytoskeleton-associated protein (Arc/Arg3.1) regulates anxiety- and novelty-related behaviors. Genes Brain Behav. *18*, e12561.

30. Heroux, N.A., Horgan, C.J., Pinizzotto, C.C., Rosen, J.B., and Stanton, M.E. (2019). Medial prefrontal and ventral hippocampal contributions to incidental context learning and memory in adolescent rats. Neurobiol. Learn. Mem. *166*, 107091.

31. Duester, K.C. (2001). Avocado fruit is a rich source of beta-sitosterol. J. Am. Diet. Assoc. *101*, 404–405.

32. Plat, J., Baumgartner, S., Vanmierlo, T., Lütjohann, D., Calkins, K.L., Burrin, D.G., Guthrie, G., Thijs, C., Te Velde, A.A., Vreugdenhil, A.C.E., et al. (2019). Plant-based sterols and stanols in health & disease: "Consequences of human development in a plant-based environment?". Prog. Lipid Res. *74*, 87–102.

33. Chen, Z.Y., Jing, D., Bath, K.G., Ieraci, A., Khan, T., Siao, C.J., Herrera, D.G., Toth, M., Yang, C., McEwen, B.S., et al. (2006). Genetic variant BDNF (Val66Met) polymorphism alters anxiety-related behavior. Science *314*, 140–143.

34. Dulawa, S.C., Holick, K.A., Gundersen, B., and Hen, R. (2004). Effects of chronic fluoxetine in animal models of anxiety and depression. Neuropsychopharmacology *29*, 1321–1330.

35. Samuels, B.A., and Hen, R. (2011). Novelty-Suppressed Feeding in the Mouse. In Mood and Anxiety Related Phenotypes in Mice: Characterization Using Behavioral Tests, T.D. Gould, ed. (Totowa, NJ: Humana Press), pp. 107–121.

36. Park, J., and Moghaddam, B. (2017). Impact of anxiety on prefrontal cortex encoding of cognitive flexibility. Neuroscience *345*, 193–202.

37. Zhou, Q.G., Zhu, X.H., Nemes, A.D., and Zhu, D.Y. (2018). Neuronal nitric oxide synthase and affective disorders. IBRO Rep. *5*, 116–132.

38. Gao, S.F., Lu, Y.R., Shi, L.G., Wu, X.Y., Sun, B., Fu, X.Y., Luo, J.H., and Bao, A.M. (2014). Nitric oxide synthase and nitric oxide alterations in chronically stressed rats: a model for nitric oxide in major depressive disorder. Psychoneuroendocrinology *47*, 136–140.

39. Pereira, V.S., Romano, A., Wegener, G., and Joca, S.R. (2015). Antidepressant-like effects induced by NMDA receptor blockade and NO synthesis inhibition in the ventral medial prefrontal cortex of rats exposed to the forced swim test. Psychopharmacology (Berl.) *232*, 2263–2273.

40. Silva, M., Aguiar, D.C., Diniz, C.R., Guimarães, F.S., and Joca, S.R. (2012). Neuronal NOS inhibitor and conventional antidepressant drugs attenuate stress-induced fos expression in overlapping brain regions. Cell. Mol. Neurobiol. *32*, 443–453.

41. Baudry, A., Pietri, M., Launay, J.M., Kellermann, O., and Schneider, B. (2019). Multifaceted Regulations of the Serotonin Transporter: Impact on Antidepressant Response. Front. Neurosci. *13*, 91.

42. Scanlon, S.M., Williams, D.C., and Schloss, P. (2001). Membrane cholesterol modulates serotonin transporter activity. Biochemistry *40*, 10507–10513.

43. Casarotto, P.C., Girych, M., Fred, S.M., Kovaleva, V., Moliner, R., Enkavi, G., Biojone, C., Cannarozzo, C., Sahu, M.P., Kaurinkoski, K., et al. (2021). Antidepressant drugs act by directly binding to TRKB neurotrophin receptors. Cell *184*, 1299–1313.e19.

44. McIntyre, R.S., Soczynska, J.K., Konarski, J.Z., and Kennedy, S.H. (2006). The effect of antidepressants on lipid homeostasis: a cardiac safety concern? Expert Opin. Drug Saf. *5*, 523–537.

45. Fjukstad, K.K., Engum, A., Lydersen, S., Dieset, I., Steen, N.E., Andreassen, O.A., and Spigset, O. (2016). Metabolic Abnormalities Related to Treatment With Selective Serotonin Reuptake Inhibitors in Patients With Schizophrenia or Bipolar Disorder. J. Clin. Psychopharmacol. *36*, 615–620.

46. Luo, X., Su, P., and Zhang, W. (2015). Advances in Microalgae-Derived Phytosterols for Functional Food and Pharmaceutical Applications. Mar. Drugs *13*, 4231–4254.

47. Silbernagel, G., Baumgartner, I., and März, W. (2015). Cardiovascular Safety of Plant Sterol and Stanol Consumption. J. AOAC Int. *98*, 739–741.

48. Katan, M.B., Grundy, S.M., Jones, P., Law, M., Miettinen, T., and Paoletti, R.; Stresa Workshop Participants (2003). Efficacy and safety of plant stanols and sterols in the management of blood cholesterol levels. Mayo Clin. Proc. *78*, 965–978.

49. Vanmierlo, T., Rutten, K., van Vark-van der Zee, L.C., Friedrichs, S., Bloks, V.W., Blokland, A., Ramaekers, F.C., Sijbrands, E., Steinbusch, H., Prickaerts, J., et al. (2011). Cerebral accumulation of dietary derivable plant sterols does not interfere with memory and anxiety related behavior in Abcg5-/- mice. Plant Foods Hum. Nutr. *66*, 149–156.

50. Aguirre-Hernández, E., Rosas-Acevedo, H., Soto-Hernández, M., Martínez, A.L., Moreno, J., and González-Trujano, M.E. (2007). Bioactivity-guided isolation of beta-sitosterol and some fatty acids as active compounds in the anxiolytic and sedative effects of Tilia americana var. mexicana. Planta Med. *73*, 1148–1155.

51. Zhao, D., Zheng, L., Qi, L., Wang, S., Guan, L., Xia, Y., and Cai, J. (2016). Structural Features and Potent Antidepressant Effects of Total Sterols and β-sitosterol Extracted from Sargassum horneri. Mar. Drugs *14*, E123.

52. Yin, Y., Liu, X., Liu, J., Cai, E., Zhao, Y., Li, H., et al. (2018). The effect of beta-sitosterol and its derivatives on depression by the modification of 5-HT, da and GABA-ergic systems in mice. RSC Advances *8*, 671–680.

53. Dagan, S.Y., Tsoory, M.M., Fainzilber, M., and Panayotis, N. (2016). COLORcation: A new application to phenotype exploratory behavior models of anxiety in mice. J. Neurosci. Methods *270*, 9–16.

54. Walf, A.A., and Frye, C.A. (2007). The use of the elevated plus maze as an assay of anxiety-related behavior in rodents. Nat. Protoc. *2*, 322–328.

55. David, D.J., Samuels, B.A., Rainer, Q., Wang, J.W., Marsteller, D., Mendez, I., Drew, M., Craig, D.A., Guiard, B.P., Guilloux, J.P., et al. (2009). Neurogenesis-dependent and -independent effects of fluoxetine in an animal model of anxiety/depression. Neuron *62*, 479–493.

56. Panayotis, N., Pratte, M., Borges-Correia, A., Ghata, A., Villard, L., and Roux, J.C. (2011). Morphological and functional alterations in the substantia nigra pars compacta of the Mecp2-null mouse. Neurobiol. Dis. *41*, 385–397.

57. Kim, D., Pertea, G., Trapnell, C., Pimentel, H., Kelley, R., and Salzberg, S.L. (2013). TopHat2: accurate alignment of transcriptomes in

the presence of insertions, deletions and gene fusions. Genome Biol. *14*, R36.

58. Anders, S., Pyl, P.T., and Huber, W. (2015). HTSeq–a Python framework to work with high-throughput sequencing data. Bioinformatics *31*, 166–169.
59. Love, M.I., Huber, W., and Anders, S. (2014). Moderated estimation of fold change and dispersion for RNA-seq data with DESeq2. Genome Biol. *15*, 550.
60. Dobin, A., Davis, C.A., Schlesinger, F., Drenkow, J., Zaleski, C., Jha, S., Batut, P., Chaisson, M., and Gingeras, T.R. (2013). STAR: ultrafast universal RNA-seq aligner. Bioinformatics *29*, 15–21.
61. Cohen, S.A., and Michaud, D.P. (1993). Synthesis of a fluorescent derivatizing reagent, 6-aminoquinolyl-N-hydroxysuccinimidyl carbamate, and its application for the analysis of hydrolysate amino acids via high-performance liquid chromatography. Anal. Biochem. *211*, 279–287.

STAR★METHODS

KEY RESOURCES TABLE

REAGENT or RESOURCE	SOURCE	IDENTIFIER
Antibodies		
c-Fos (rabbit polyclonal)	Genetex	Cat# GTX129846
Alexa Fluor 488 secondary antibody (Donkey anti-rabbit)	Thermo Fisher Scientific	RRID: AB_2556546
Alexa Fluor 546 secondary antibody (Donkey anti-rabbit)	Thermo Fisher Scientific	RRID: AB_2534016
DAPI (4.6-diamino-2-phenolindol dihydrochloride)	Thermo Fisher Scientific	RRID: AB_2629482
Chemicals, peptides, and recombinant proteins		
β-sitosterol	Sigma-Aldrich	Cat# S1270
Stigmasterol	Sigma-Aldrich	Cat# S2424
Brassicasterol	Sigma-Aldrich	Cat# B4936
Fucosterol	Sigma-Aldrich	Cat# F5379
Campesterol	Chemos	Cat# A0004730
Fluoxetine hydrochloride	Sigma-Aldrich	Cat# F132
Fluspirilene	Sigma-Aldrich	Cat# F100
Oxamniquine	BOC Sciences	Cat# 21738-42-1
Alvespimycin	InvivoGen	Cat# ant-dlg-5
Primaquine diphosphate	Prestwick Chemical	Cat# Prestw-476
Corn oil	Sigma-Aldrich	Cat# 8001-30-7
DMSO (Dimethyl sulfoxide)	Sigma-Aldrich	Cat# D2650
L-Norleucine	Sigma-Aldrich	Cat# N-8513
L-Arginine-13C6	Cambridge Isotope Laboratories	Cat# CLM-2265-H-0.05
Norepinephrine-D6	CDN Isotopes	Cat# D6634
Dopamine-D4	CDN Isotopes	Cat# D1550
Serotonin-D4	Sigma-Aldrich	Cat# 73483
Amino acid standard mix	Sigma-Aldrich	Cat# A-9906
Epinephrine	Sigma-Aldrich	Cat# E4375
Dopamine	Fluka	Cat# 56610
Serotonin	Sigma-Aldrich	Cat# H9523
6-aminoquinoline	Sigma-Aldrich	Cat# 275581
N,N'-Disuccinimidyl carbonate	Sigma-Aldrich	Cat# 43720
Acetonitrile ULC/MS	Bio-Lab	Cat# 012041
Formic acid ULC/MS	Bio-Lab	Cat# 069141
Perchloric acid	Sigma-Aldrich	Cat# 311413
Critical commercial assays		
RNA extraction kit: RNAqueous-Micro Kit	Ambion / Life Technologies Corp.	Cat# AM1931
Deposited data		
Expression profiling by high throughput sequencing	GEO (Gene Expression Omnibus) database	GEO: GSE134633
Experimental models: Organisms/strains		
Mouse / C57BL/6OlaHsd	Harlan Israel	N/A
Software and algorithms		
Ethovision XT 13	Noldus	RRID: SCR_000441
VideoMot2	TSE Systems	RRID: SCR_014334

(*Continued on next page*)

Continued

REAGENT or RESOURCE	SOURCE	IDENTIFIER
COLORcation	Fainzilber lab (Dagan et *al*., 2016)	N/A
Prism v8 for Windows	GraphPad Software, La Jolla, California, USA	RRID: SCR_002798
Fluoview FV10-ASW 4.1	Olympus	RRID: SCR_014215
Fiji	NIH	RRID:
MassLynx 4.1	Waters	RRID: SCR_014271
TargetLynx XS	Waters	https://www.waters.com/waters/en_IL/TargetLynx-/nav.htm?cid=513791&locale=en_IL
Other		
Fluoromount-G® (mounting solution)	SouthernBiotech	Cat# 0100-01

RESOURCE AVAILABILITY

Lead contact

Further information and requests for resources and reagents should be directed to and will be fulfilled by the lead contact, Nicolas Panayotis (nicolas.panayotis@weizmann.ac.il)

Materials availability

All data and materials that support the findings of this study are available from the Lead Contact without restriction. This study did not generate new unique reagents.

Data and code availability

Gene expression analysis (RNA-seq) data generated from this paper have been deposited in NCBI's Gene Expression Omnibus (GEO) and are accessible through GEO series accession number GEO: GSE134633.

EXPERIMENTAL MODEL AND SUBJECT DETAILS

Animal subjects

C57BL/6J mice were purchased from Envigo (Israel). Mice were kept at 24.0 ± 0.5°C in a humidity-controlled room under a 12-hr light-dark cycle with free access to food and water. Experiments were carried out on 2 to 5 months-old male mice unless specified otherwise.

Study approval

All procedures involving animal subjects were approved by the IACUC of the Weizmann Institute of Science and carried out in line with the European Union directive 2010/63/EU for the care and use of laboratory animals.

METHOD DETAILS

Pharmacological treatments

All drugs were administered by intraperitoneal injection (i.p.) or oral gavage. The following plant sterols were purchased from Sigma-Aldrich: β-sitosterol (Cat#S1270), stigmasterol (Cat#S2424), brassicasterol (Cat#B4936), and fucosterol (Cat#F5379). Campesterol was purchased from Chemos, Germany (Cat#A0004730). All these hydrophobic compounds were dissolved in corn oil (Sigma-Aldrich, Cat#C8267). Fluspirilene (Sigma-Aldrich, Cat#F100) was dissolved in PBS containing 10% DMSO. Alvespimycin (17-DMAG, InvivoGen, Cat#ant-dlg-5) and Oxamniquine (BOC Sciences, Cat#21738-42-1) were dissolved in saline solution. Fluoxetine (Fluoxetine hydrochloride, Sigma-Aldrich, #F132) was dissolved in saline solution. The latter drug was used as a serotonin reuptake inhibitor (SSRI) and anxiety-reducing properties were tested after three weeks of treatment[33].

Behavioral analysis

Behavioral testing was performed during the ''dark'' (i.e., active) phase of the diurnal cycle; the ventilation system in the test rooms provided a ~65 dB white noise background. Every daily session of testing started with a 1 hr habituation period to the test rooms. A recovery period of at least 1 day was provided between the different behavioral assays.

Chronic restraint stress

Mice were physically restrained in 50 ml ventilated Falcon tubes for 1.5 hours/day (during midday time), for three weeks. Control mice (naive), were housed in their usual cages under normal conditions.

Open field test

The apparatus for the open-field test (TSE System, Germany) consisted of a 120 lx-illuminated white Plexiglas box (50 cm × 50 cm × 40 cm). The test relies on the natural conflict of a rodent between the exploration of a novel environment and the aversive properties of a large, brightly lit area. Each mouse was placed in the corner of the apparatus to initiate a 10-min test session. A camera mounted above the apparatus transmitted images of the mouse. Motility and anxiety-like behaviors were assayed as in our previous work[12]. The total distance moved (cm), the time spent (global, center, border; s), center/border ratio, movement velocity (cm/s), and percentage of time spent moving versus rest in the different defined area were recorded using the VideoMot2 software (TSE System, Germany). Open-field raw data were then analyzed with *COLOR*cation[53], allowing the unbiased study of mice activity based on group heat-maps.

Elevated plus maze

The EPM contains two open arms and two enclosed ones (with walls) connected by a central square. Exploration on the open arms is reduced in high anxiety states while it is increased in low anxiety states[54]. Mice were placed on the central platform facing one of the open arms to initiate a 5-minute test session and the distance and time spent in each arm were measured. The procedure and mouse tracking were conducted using Noldus EthoVision XT13 software, as previously described[12].

Contextual fear conditioning

The contextual fear conditioning paradigm was used to study possible alteration of hippocampal forms of memories. The procedure and mouse tracking were conducted using Noldus EthoVision XT13 software while measuring freezing behavior, defined here as a lack of movement (excluding respiration, freezing bouts duration, 3 s). The test was performed within three days, as follows. On the first day, mice are habituated for 5 min to the fear conditioning chamber, a clear Plexiglas cage (21 cm × 20 cm × 36 cm) with a stainless steel floor grid within a constantly illuminated (120 lx) fear-conditioning housing. Conditioning then takes place on the second day in one 5-min training session. Mice initially explore the context for two min. Thereafter, two pairings of a co-terminating tone [conditioned stimulus (CS): 30 s, 3,000 Hz, pulsed 10 Hz, 80 dB (A)] and shock [unconditioned stimulus (US): 0.7 mA, 2 s, constant current) with a fixed ITI of 60 s were delivered. The US was delivered through the metal grid floor. Mice were removed from the chamber one min after the last CS-US pairing. The chamber was cleaned with 10% ethanol before each session. Constant auditory background noise was delivered from an audio file by speakers located in the chamber [white noise, 62 dB(A)]. Finally, context-dependent memory was tested 24 hr after conditioning by re-exposure to the conditioning box for 5 min without any stimuli.

Novelty-suppressed feeding

The task assesses the ability of the animal to resolve a conflict between a context that induces heightened anxiety and a drive to approach an appetitive stimulus. Testing was carried out in the open field arena, set up under bright lighting conditions (~1000 lux). The open field is positioned under a digital camera connected to a computer equipped with the Noldus MediaRecorder software. The protocol followed the recommendations of previous studies[35,55]. Briefly, a piece of white filter paper was placed in the center of the arena with a small piece of rodent chow. For this task mice were food-restricted for a period of 24 hours. After food restriction, the test consists of placing the animals in the brightly lit open field and measuring the time to approach and eat a pellet of food located in the center of the arena. Latency to approach and eat are used to measure anxiety-like behavior (a cut-off time of 600 s was used in our experiment).

Accelerated rotarod

Mice were subjected to three trials, with 5 min inter-trial intervals. During each trial, the rotarod accelerates from 4 to 40 rpm in 300 s. The latency to fall was recorded in the number of seconds. The best of the three trials was recorded. If a mouse clinging on the rod completes a full passive rotation we push down the lever and record the latency. In this case, a passive rotation was considered as a failure in performance similar to falling[56].

Heat probe test

We investigated responses to noxious heat using the heat probe test by applying a metal probe heated to 58°C to a hindlimb paw while holding the animal. Paw withdrawal latency was timed (typically ranging between 2-4 s in wild-type animals). The test was repeated three times for each animal, with at least 20 minutes intervals between repeats, as previously described[13].

von Frey test

von Frey tests of sensitivity to mechanical stimuli were conducted as previously described[13]. Briefly, mice were placed in acrylic chambers suspended above a wire mesh grid and allowed to habituate to the testing apparatus for one hour before experimentation. When the mouse was calm, the von Frey filaments were pressed against the plantar surface of the paw until the filament buckled. A

positive response was noted if the paw was sharply withdrawn upon application of the filament. Testing begins with a filament's target force of 13.7 milliNewtons and progresses according to an up-down method.

RNA expression analysis (RNA-seq)

We carried out RNA-seq analyses to assess the impact of β-sitosterol or stigmasterol administration on the hippocampal transcriptome. Total RNA was extracted from hippocampi dissected from C57BL6 wild-type animals treated with vehicle (corn oil), β-sitosterol, or stigmasterol at 100 mg/kg of body weight, using the RNAqueous-Micro Kit (Ambion) according to manufacturer's instructions. Intraperitoneal injections of the vehicle or drug were done 1 hr prior to dissection. There were 4 and 3 replicates per group for β-sitosterol and stigmasterol, respectively. Replicates of high RNA integrity (RIN R > 7) were processed for RNA-Seq at the Crown Institute for Genomics (G-INCPM, Weizmann Institute of Science). 500 ng of total RNA for each sample was processed using the TruSeq RNA sample preparation Kit v2 protocol (Illumina). Libraries were evaluated by Qubit and TapeStation. The data was analyzed using DESeq software and has been deposited in NCBI's Gene Expression Omnibus (GEO accession number: GSE134633).

Library construction and sequencing

Library construction

Sequencing Libraries were constructed with barcodes to allow multiplexing of 16 samples (β-sitosterol) or 12 samples (stigmasterol) on 2 lanes of Illumina HiSeq machine, using the Single Read 60 protocol (v4). The output was ~34.8 million reads per sample (β-sitosterol experiment) and ~45 million reads per sample (stigmasterol experiment). Fastq files for each sample were generated by the usage of Illumina CASAVA 1.8.2 software (β-sitosterol experiment) and bcl2fastq-v2.17.1.14 (stigmasterol experiment).

Sequence data analysis

β-sitosterol injection

Poly-A/T stretches and Illumina adapters were trimmed from the reads using cutadapt (1); resulting reads shorter than 40 bp were discarded. Reads for each sample were aligned independently to the *Mus musculus* reference genome GRCm38 using TopHat2 (v2.0.10)[57] with default parameters. The percentage of the reads that were aligned uniquely to the genome was ~92.5%. Counting proceeded over genes annotated in Ensembel release 82 using htseq-count (version 0.6.1p1)[58]. Only uniquely mapped reads were used to determine the number of reads falling into each gene (intersection-strict mode). Differential analysis was performed using DESeq2 package (1.6.3)[59] with the betaPrior, cooksCutoff, and independentFiltering parameters set to False. Raw *P values* were adjusted for multiple comparisons using the Benjamini and Hochberg procedure. Differentially expressed genes, were determined by a *P*-adj of < 0.05, absolute fold changes > 1.5 and max raw counts > 30.

Stigmasterol injection

Poly-A/T stretches and Illumina adapters were trimmed from the reads using cutadapt; resulting reads shorter than 30bp were discarded. Reads for each sample, were aligned independently to the *Mus musculus* reference genome GRCm38 using STAR (2.4.2a)[60], supplied with gene annotations downloaded from Ensembl (and with EndToEnd option). The percentage of the reads that were aligned uniquely to the genome was ~89.5%. Counting proceeded over genes annotated in Ensembel release 92 using htseq-count (version 0.6.1p1)[58]. Only uniquely mapped reads were used to determine the number of reads falling into each gene (intersection-strict mode). Differential analysis was performed using the DESeq2 package (1.10.1)[59] with the betaPrior, cooksCutoff, and independentFiltering parameters set to False. Raw *P values* were adjusted for multiple comparisons using the Benjamini and Hochberg procedure. Differentially expressed genes, were determined by a *P*-adj of < 0.05, absolute fold changes > 1.5 and max raw counts > 30.

Bioinformatics analysis

K-Means clustering using Pearson's dissimilarity was performed. Standardized, $\log_2$ normalized counts were used for the clustering analysis. Clustering analysis was performed with Rstudio v3.2.1.

Differentially expressed (DE) genes were analyzed using the Ingenuity Pathways Analysis (Ingenuity® Systems, https://digitalinsights.qiagen.com/) suite to determine the most significant and biologically relevant functions and pathways.

Connectivity Map analysis

The Broad Institute Connectivity Map (CMap, https://clue.io/cmap) is a database with a collection of gene expression profiles that are obtained from cultured human cell lines treated with small pharmacological compounds[15]. We queried CMap (CMap_build02) with up and downregulated gene lists from wild-type versus importin α5 knockout hippocampi (GEO accession number GSE106546). CMap then scored the similarity of the up and down lists with the deposited expression profiles. As a result, the similarity of the transcriptional responses is scored for each small molecule. An enrichment score of "1" indicates a perfect correlation, where genes in the up-list are upregulated and the genes in the down-list are downregulated in a CMap microarray data. Because our RNA-seq data were obtained from mouse samples, and CMap data are obtained from human cell lines with the Affymetrix HG-U133A microarray chip, we used a custom-made MATLAB script to convert the mouse gene identifiers to their human orthologs gene identifiers.

Immunofluorescence

We used immunofluorescence to assess the level of c-Fos expression. Mice were euthanized by cervical dislocation (without pharmacological anesthesia) 1 hour after contextual fear conditioning. Brains harvested for immunostaining were post-fixed for 5 h and cryoprotected in 20% sucrose for 24 h, then frozen at −80°C before cryostat sectioning (20 μm coronal sections). Slices containing sections of the cortex (prefrontal cortex), hippocampus (dorsal), and amygdala were collected in separate sets for immunohistochemistry so that each set contained every fifth serial section. Briefly, sections were rehydrated (PBS 1X), permeabilized (0.1% Triton X-100 PBS 1X), blocked (7% normal donkey serum), and incubated overnight at room temperature with Rabbit anti-c-Fos (1:1000, GeneTex, GTX129846). Sections were subsequently incubated with donkey anti-rabbit secondary antibody (Alexa 488 or Alexa 546), DAPI (4',6-diamino-2-phenolindol dihydrochloride), counterstaining was performed on all sections to visualize the nucleus, and the sections were mounted with Fluoromount-G® (SouthernBiotech, Cat#0100-01).

Image processing and quantification

Images were acquired on an Olympus FV1000 inverted confocal (Olympus, Tokyo) with Fluoview (FV10–ASW 4.1) software. In general, brain slices were scanned using camera settings identical for all groups/treatments in a given experiment. Images were imported into the Fiji version (https://fiji.sc/.) of the ImageJ software for threshold subtraction and subsequent analyses (see below).

Quantification of c-Fos positive neurons

For the detection of c-Fos-positive cells, images were analyzed with the Fiji software (http://fiji.sc). Brain areas such as the medial prefrontal cortex (mPFC), the dentate gyrus (DG), CA3 field of the dorsal hippocampus (dCA3), and the basolateral amygdala (BLA) were identified based on the DAPI signal following the Paxinos and Franklin mouse brain atlas. c-Fos-positive cells were counted within the outlined structures and their density (c-Fos+ cells/mm^2) averaged over 2–5 sections per animal.

Neurochemical measurements

Materials

Acetonitrile and formic acid of ULC/MS grade were from Bio-Lab (Israel). Water at 18.2 MΩ resistance was obtained using a Direct 3-Q UV system (Millipore). Mix of amino acid standards and neurotransmitters from Sigma-Aldrich was used. Norepinephrine-D6 (NEN-D6), dopamine-D4 (DA_D4), serotonin-D4 (5-HT-D4), L-arginine-13C6 (Arg-13C6), and L-norleucine (NorLeu) were used as internal standards (IS).

Extraction

The extraction procedure was performed at 4°C. Pre-weighted samples in 1.5-mL test tubes were spin shortly (21,000 g, 15 s) to place them at the bottom. Fifty μL of 4% perchloric acid containing IS mix (NorLeu 2uM; Arg-13C6 12uM; NEN-D6 20ng/ml; DA-D4 40ng/ml; ST-D4 400ng/ml) was added and the mixture was homogenized using a handheld grinder (Agros), followed by agitation in a shaker (1200 rpm, 30 min, ThermoMixer C, Eppendorf) and centrifuged (20,000 g, 10 min). The collected supernatants were used for further analysis.

Derivatization

Derivatization procedure was performed using AQC reagent synthesized as described[61]. Briefly, a 10 μL aliquot of the sample or standard solution (with the internal standards added) and 70 μL of 0.15 M sodium borate solution, pH 8.8 were derivatized with 20 μL of AQC in acetonitrile (2.7mg/mL) by heating at 55°C for 10 min. The reaction mixtures were cooled and placed in nanofilter vials (Thomson, 0.2um PES) for LC-MS.

LC-MS/MS analysis

The LC-MS/MS instrument consisted of Acquity I-class UPLC system (Waters) and Xevo TQ-S triple quadrupole mass spectrometer (Waters) equipped with an electrospray ion source and operated in positive ion mode was used for analysis. MassLynx and TargetLynx software (v.4.1, Waters) was used for the acquisition and analysis of data. Chromatographic separation was done on a 150 × 2.1-mm i.d. 1.8-μm UPLC HSS T3 column equipped with 50 × 2.1-mm i.d., 1.8-μm UPLC HSS T3 pre-column (both Waters Acquity) with 0.1% formic acid as mobile phase A and 0.1% formic acid in acetonitrile as B at a flow rate of 0.6 ml/min and column temperature 45°C. A gradient was as follows: 0.5 min the column was held at 4%B, then linear increase to 10%B in 2 min, then to 28%B in 2.5 min, and to 95%B in 0.1 min. Just after back to 0%B during 1.1 min, and equilibration at 4%B for 1.3 minutes. Samples kept at ambient temperature (23°C) were automatically injected in a volume of 1 μl. For mass spectrometry argon was used as the collision gas with 0.10 ml/min flow. The capillary voltage was set to 3.00 kV, cone voltage 25V, source offset 30V, source temperature 150°C, desolvation temperature 650°C, desolvation gas flow 800 L/hr, cone gas flow 150 L/hr. Analytes were detected using corresponding selected reaction monitoring (SRM) and retention times as shown in the Table S4. The concentrations based on standard curves were calculated using TargetLynx (Waters). Multiple Reaction Monitoring (MRM) parameters are reported in the Table S4.

QUANTIFICATION AND STATISTICAL ANALYSIS

Data collection

No statistical methods were used to predetermine sample sizes, but they were similar to those reported in previous publications. Data collection and analysis were performed blind to the conditions of the experiment. All mice were randomly assigned to the different experimental conditions.

Statistics

A normality test (Shapiro-Wilk test) was applied to all data before analysis for statistical significance. Datasets that passed the normality test were subjected to parametric analysis. For 2-group analyses, an unpaired Student's t test was used. Analysis of multiple groups was made using the ANOVA method. The choice between one- or two-way ANOVA was based on the requirements for identification of specific factors' contribution to statistical differences between groups and were followed as specified in the figure legends by the Tukey, the Sidak, or the Dunnett's post hoc analysis tests. Datasets that did not pass the normality test were subjected to the Mann-Whitney or the Kruskal-Wallis test followed by Dunn's multiple comparisons test. In the NSF test, we used the Kaplan-Meier survival analysis due to the lack of normal distribution of the data. The Mantel-Cox log-rank test was used to evaluate differences between experimental groups. Potential outliers were identified and discarded using the ROUT method with a Q (maximum desired false discovery rate) of 1%. All analyses were performed using GraphPad Prism version 8.00 for Windows (GraphPad Software, La Jolla, California, USA, https://www.graphpad.com/). All statistical parameters and *P*-values for specific analyses are reported in the figure legends of the paper.